EEIG
Route de Soultz
BP38
F-67250 Kutzenhausen

Short Note on

1^{st} Stimulation Phase of GPK4

During 13-16 September 2004:

Prognosis and Conclusion

Technical Note
September 2004

Ref. 017.5 TK/TM

24. September 2004

GEOWATT AG
SWISS GEOTHERMAL EXPERT GROUP
GEOWATT AG
Dohlenweg 28
CH-8050 Zürich
Tel +41 (0) 1 242 14 54
Fax +41 (0) 1 242 14 58
info@geowatt.ch
www.geowatt.ch

1 BACKGROUND

The new hydraulic stimulation tool HEX-S has been recently developed. It is originally based upon the combination of two well-experienced codes: FracSim3D from Willis-Richards et al. (1996) and extended by Jing et al. (1998) and the FE code FRACTure (Kohl & Hopkirk 1995). Before integrating both parts into HEX-S major development steps preceded: on the mechanical fracture behaviour fracture and fault zones can be split into arbitrary slip patches and a GUI interface allows now to define physical parameters of various fractures and to visualize the imposed shear events (Bächler et al. 2001, Kohl et al. 2004). The 3D numerical FE implementation is performed by a completely new hydraulic implementation accounting for the mapping of individual fracture sets onto the grid elements. The mapping is performed from deterministic and stochastic fracture sets that are derived from borehole observations and stochastic parameters evaluation. As a gross number, sets of >20'000 single fractures are generated and accounted for. During the modeling procedure more hydraulic features such as fault zones not intersecting the borehole can be included in the data treatment (Kohl et al. 2004).

The goal of the modeling with HEX-S is to provide a reliable physical explanation of the hydraulic and seismic events during hydraulic stimulation. Various theoretical test scenarios have been calculated already, however, this time the challenging task of a prognosis was intended.

2 SOULTZ GPK4 STIMULATION

Successful model runs have been performed on the GPK3 data of the stimulation test 03may27 from an earlier phase at the Soultz EGS. Hereby, both the early development of the seismic cloud (t<1-2 days) and of the downhole pressure have been qualitatively explained (publication under way). Based on this experience, the stimulation of GPK4 should be explained by two models:

- A prognosis model, based on the UBI data from GPK4 and on the hydraulic conditions revealed by the low injection test (0.7l/s over several days).
- A conclusive model accounting for the seismic and hydraulic stimulation results.

The calculations are based on different model assumptions. The basis is a FE grid consisting of ~400'000 nodes that includes the open hole sections of GPK2, GPK3 and GPK4. In the modeling procedure, vertical boreholes had been assumed, each located near the top of the corresponding open hole section. The deviations to the real trajectories of GPK2 and GPK3 are minor, with the exception of a lateral difference of ~100 m for the bottom part of GPK4. Accordingly, the observed locations of the fractures at this part of GPK4 have been corrected for the deterministic fracture data. The flow in the matrix is assumed to be oriented towards the lateral boundaries. To best represent the influence of strongly vertically oriented far-field drainage systems, Dirichlet boundary conditions were placed at min. ~5 km distance from each borehole.

Earlier sensitivity calculations for the GPK3 stimulation have revealed the high sensitivity of our model assumptions to the stress field. Initially, a transfer from a normal stress regime (σ_V being the main stress component) to a strike-slip regime (σ_H being the main stress component) at ~4500m has been assumed. Given the fracture distributions and orientations at all boreholes, many fracture sets would fail already at minor hydraulic pressure variations. Even a vague fit of the seismic observations couldn't be obtained. However, a much more reliable and robust situation evolved when assuming a normal stress field throughout the model depth down to 6 km. Identical behavior has been observed for the GPK4 data. Therefore all our calculations and conclusions have been based on a normal stress field.

Given the low initial injectivity at GPK4 the matrix permeability is generally assumed to be rather small, compared to general conditions at Soultz ($k=10^{-15}m^2$). The key hydraulic influence is due to the fracture distribution at each borehole. At each borehole, the apertures of the fractures are scaled to reproduce the initial hydraulic borehole transmissivity. The observed fractures intersecting the boreholes define a weighted set of orientations for the stochastic filling of the matrix with fractures up to a predefined density. Generally, the BRGM fracture borehole data were used, only at GPK4 the data from R. Maurer, our diploma student 2004, were included. Also, the same large matrix fault zones from Maurer (2004) were anticipated.

2.1 PREDICTION OF STIMULATION BEHAVIOUR

Hydraulic behavior

Given the results from the initial low-flow rate injection test 04sep08, different model calibration runs have been realized to prepare the forecast runs for the subsequent stimulation test. On 13 Sep 11:00 a rough description and conclusion from these predictive evaluations has been finalized and mailed to the Soultz project partners. Herein, only the model runs "C" will be presented that produced the most robust shearing events (see note on stress field; Model "B" assumed a stress transfer from normal to strike slip).

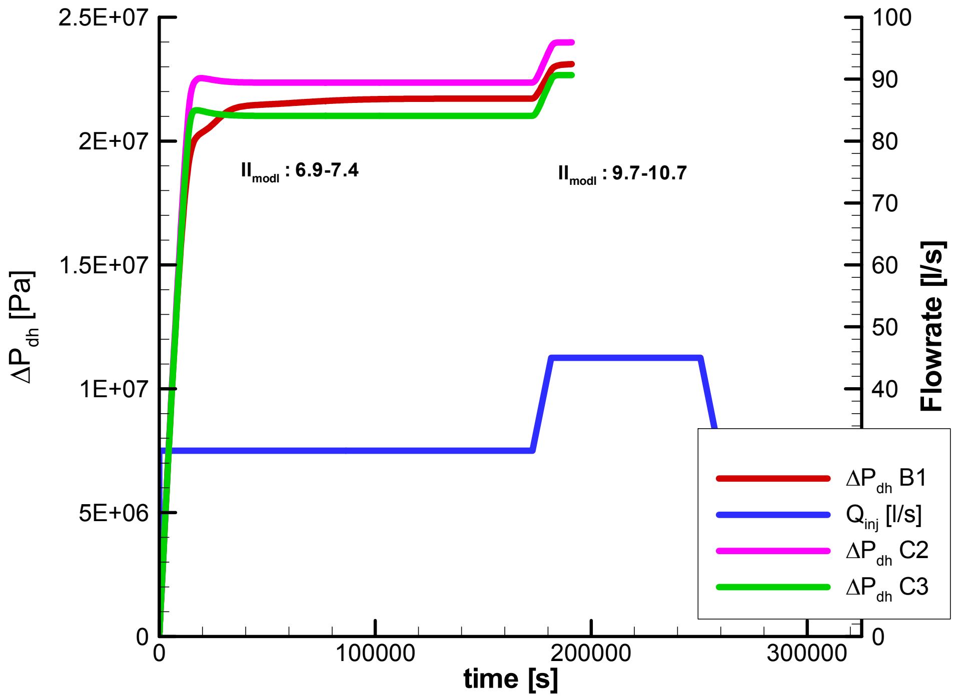

Fig. 1: Predicted hydraulic pressure development at GPK4 for a stepwise 30/45 l/s injection at GPK4. A downhole pressure increase of 21 MPa for 30l/s has been calculated, an

additional 1.5 MPa would result when increasing the injection rate to 45 l/s. For the models C2/C3 a maximum peak at the beginning occurs at t=15500 s; Model B1 (based on a slightly different geometry) would not produce any characteristic peak in the start phase. Calculations assume an instantaneous 30 l/s flow rate.

The models predicted an increase of the downhole pressure between ~20 MPa and ~24 MPa for injection rates between 30l/s and 45 l/s. Compared to the low rate injection test the increase of the injectivity was expected to be in a range of 6.9-7.4 at 30l/s and of 9.7-10.7 for 45 l/s. Therewith, higher flow rates still would significantly improve the hydraulic conditions at GPK4.

Shearing events

The shearing events were predicted to occur mostly at the bottom part of GPK4. Due to the strong inclination of GPK4, the ~100m deviation of the bottom part due to modeling restrictions requires a corresponding correction between forecasted and measured event locations.

For the first 10 hrs of the stimulation test shearing is forecasted to occur within a radius of 100 m around GPK4 at z ≈ -4900m (Δz=±75m) and extending towards greater depths. During a next time interval (t<1day), the forecasted cloud should have moved slightly upwards (+100m) and first pronounced events should spread towards the stimulated areas next to GPK3, as well as along the large matrix fault zones which do not intersect any borehole, located by Maurer (2004).

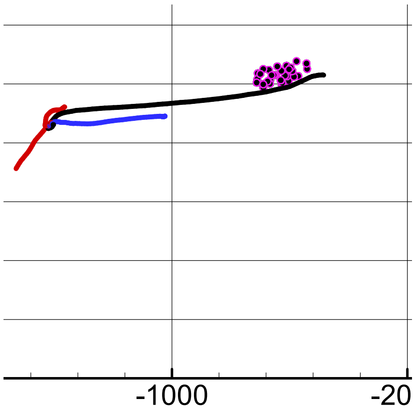

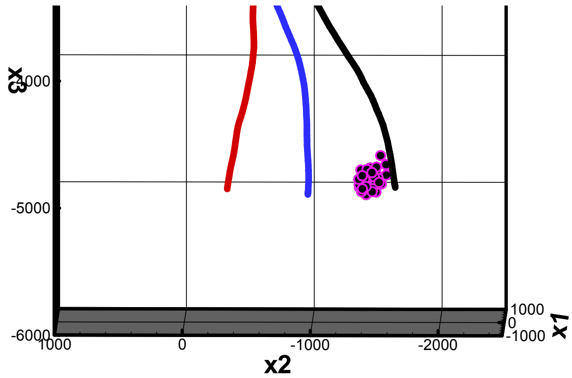

Fig. 2: Predicted microseismic evolution at GPK4 within the 1st 10h interval after stimulation start (left: plane view, right: view from west). The lines represent the real borehole locations (black GPK4, blue GPK3, red GPK2). The modeled downhole part of GPK4 is ~100m left to real GPK4 trajectory (see text). The modeled events are not location-corrected.

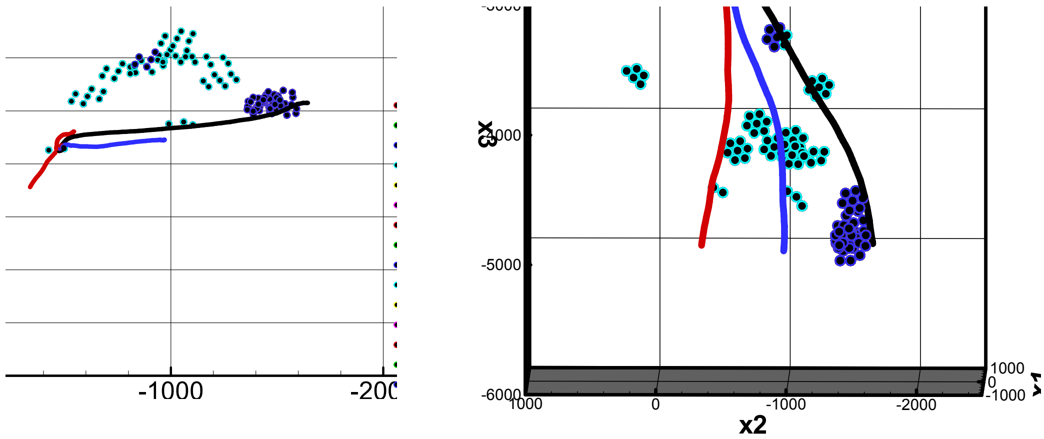

Fig. 3: Predicted microseismic evolution at GPK4 within the 1st day after stimulation begin (left: plane view, right: view from w). Compared to the 1st 10 hr interval, now, especially the assumed far field faults would start to fail. But also the events next to GPK4 would continue to migrate upward.

2.2 CONCLUSION AND INTERPRETATION

Comparison to stimulation data

The first stimulation phase has been conducted for 4 days from 13 to 16 Sep. 2004, with a general injection rate of 30 l/s. The pre-stimulation downhole pressure at 4700 m depth was ~46.2 MPa, reflecting however a declining trend due to shut-in from the earlier low-rate injection test. It can be estimated that the pressure was still ~2.8 MPa above the initial hydrostatic pressure (43.4 MPa). This level is approached by < 0.03 MPa/hr (or < 0.7 MPa/day) just before the start of the injection test. The 30 l/s injection increased the total downhole pressure at GPK4 in 4700 m depth up to 61.5 MPa within ~8000 s. After that, a pressure decline of 0.023 MPa/hr occurred that certainly is the result of the superimposed declining trend from the earlier low-rate injection. Starting 49 hr after injection begin, flow-rate was increased three times to 45 l/s over a short, 1.5 hr period. An average additional pressure increase of 1 MPa resulted from these tests.

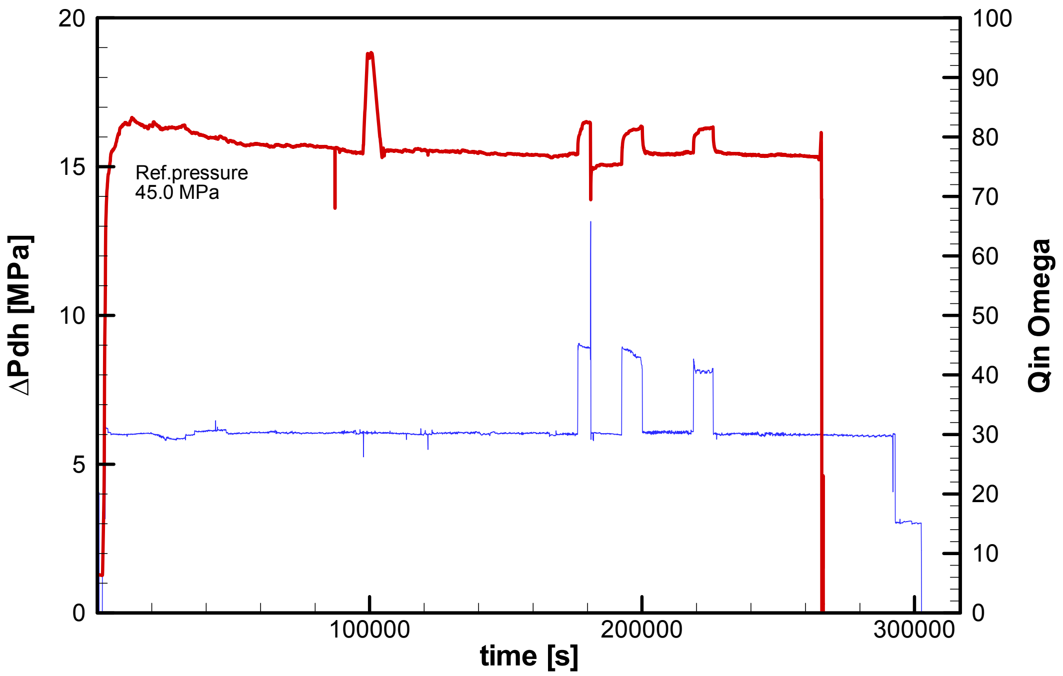

Fig. 4: Downhole pressure and flow rate during the 1st phase of stimulation in GPK4 between 13-16 Sep. 2004. Reference time (t=0) is 13 Sep 2004 08:00.

Seismic activity started at the bottom of the borehole GPK4 and gradually developed northwards towards GPK3 and upwards towards the casing shoe (Fig. 5).

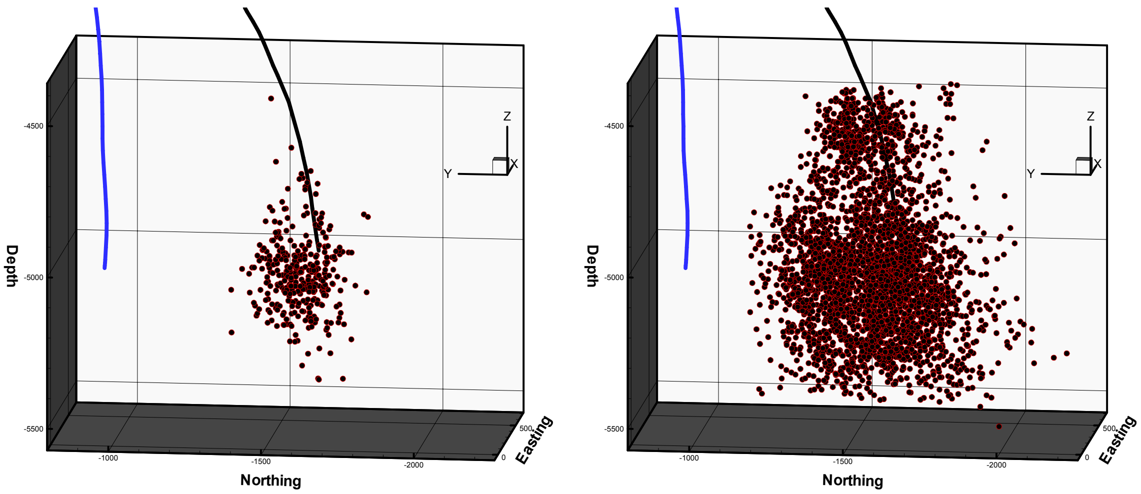

Fig. 5: Seismicity at GPK4 during the first 10 hr stimulation (left) and accumulated over the total 1st stimulation phase until 19 Sep 2004 00:00 (GPK4 black, GPK3 blue line).

Conclusion on far-field structures

In our predictive model it can be seen from the evolution of the calculated shearing events (Fig. 3) that the far-field connected fault zones play a dominant part for the further explanation of long-term stimulation behavior. In the predictive model, flow would be strongly dominated by these features at a later stimulation phase and would then be observable directly through shearing and indirectly through the hydraulic pressure development. Note, the later-on measured nearly steady-state pressure behavior has been forecasted, once it had reached a certain level – see Fig. 1.

However, the assumed far-field connected fault zones in the predictive model would result in a leakage from the stimulated fracture zones at GPK4 into fault zoned located such that a good hydraulic connection between GPK4 and the well-stimulated GPK3/GPK2 area is ensured. Clearly, the data of the GPK4 stimulation test hasn't given any clue to this flow/pressure connectivity. The pressure increased only slightly in GPK3/GPK2 with very long time constants (0.5 MPa after 3 days). These observations lead to us to newly assess the measured microseismic events, since they may (directly or indirectly) elucidate whether a far-field connected fault zones exist or not. Thereby, the focus is given to the transient evolution of seismicity and to the gradient of a new introduced parameter, the seismic density (=number of events per m^3). These considerations were derived from modeling interpretation with HEX-S for the GPK3 stimulation test. Our modeling indicates a link between the shearing events occurring in high-pressurized flow zones and neighboring low-pressurized aseismic matrix. The transient evolution of microseismicity becomes more pronounced only when an adjacent zone is opened and ready to be penetrated by flow. But also the opposite behavior can occur when unfavorably oriented (for shearing), well-conducting zones - visible only as aseismic areas - are intersected by shearing fractures. Both occurrences provide a high seismic density gradient.

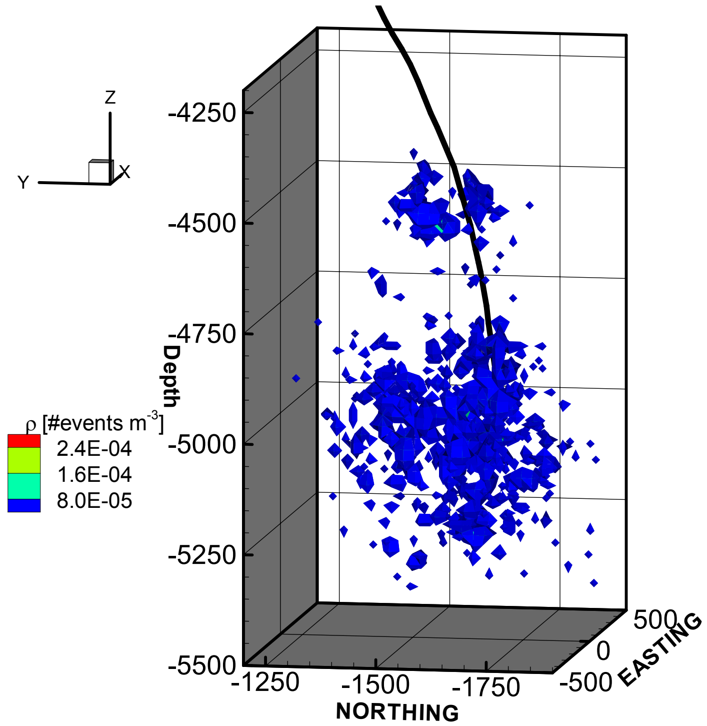

Fig. 6: Seismic density of the stimulated GPK4 events (corresponding to Fig. 5-right). Higher isosurface values are enclosed in the blue 8.10^{-5} events/m^3 surface.

The density plot shown in Fig. 6 is derived for a mesh size of 25^3 m^3. An isosurface plane with the magnitude of 8.10^{-5} events/m^3 corresponds therewith to 1.25 events per grid box.

Apart of a better spatial visibility, the density plot also offers the advantage of ignoring spurious single events.

By investigating the ensemble of microseismic events from GPK2, GPK3 and GPK4 clear boundaries and aseismic zones show up. At current, a zone between GPK3 and GPK4 might be of most interest, since it could provide a drainage system for the injected flow and could prevent pressurizing GPK3. Fig. 7 represents the total of seismic density of all located events from all stimulations. Noteworthy is the fact of a relative poor stimulation around GPK3, a fact that is in agreement with its neglecting increase of injectivity.

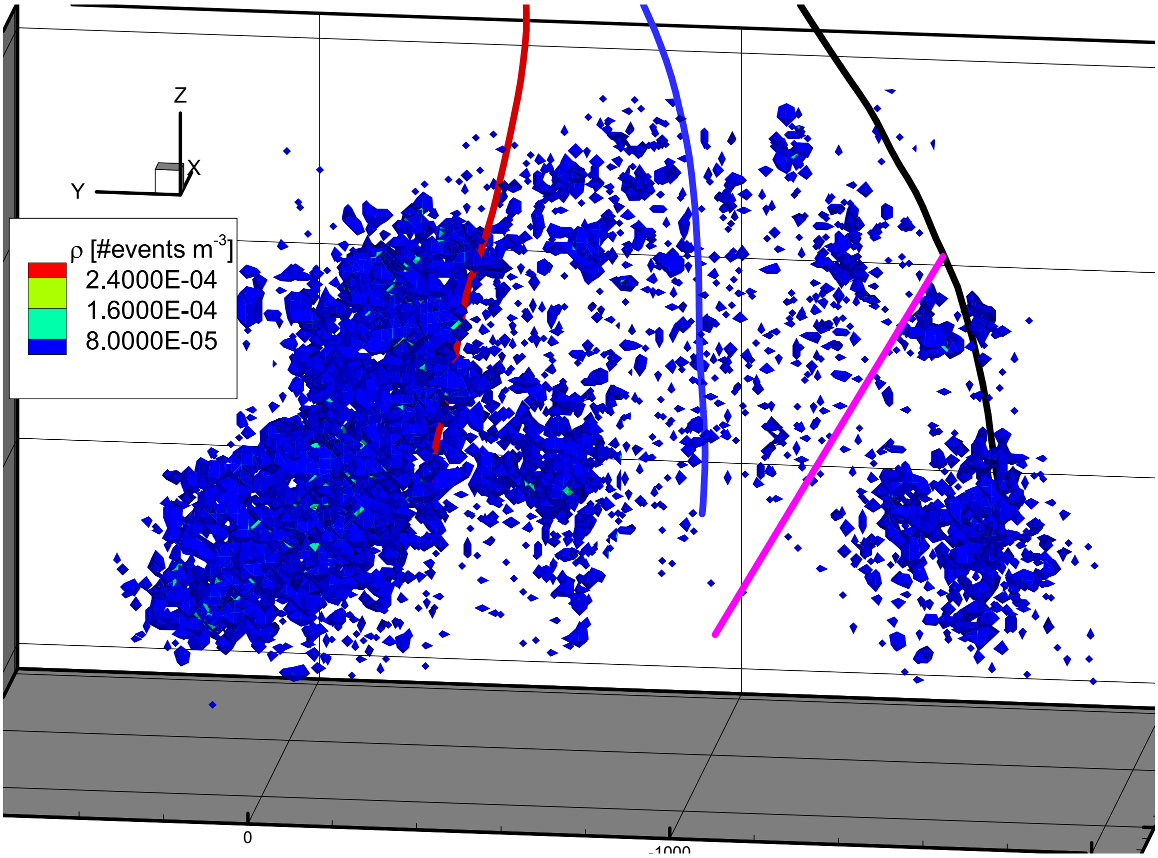

Fig. 7: Zoom at an aseismic zone between GPK3 and GPK4 (magenta line)

Especially, Fig. 7 also illustrates a roughly E-W striking aseismic zone that isn't penetrated neither by GPK3 nor by GPK4 events..

2.3 GENERAL CONCLUSION

The new hydro-mechanical reservoir simulator HEX-S is now fully operational. Its capabilities are documented for the GPK3 and GPK4 stimulation at the Soultz EGS site. Experience with GPK4 stimulation has demonstrated that the tool is especially well suited to

- forecast the early ($t < 1$ day) hydraulic and seismic behavior
- explain the major processes responsible for the induced microseismicity

The forecast resulted in an extraordinarily precise simulation of the seismic pattern, including both, spatial location and spatial evolution during the first 10 hr stimulation period. Further-on occurring differences between measured and forecasted events are due to assumptions on major far-field connected flow zones not penetrating the borehole locations. In order to improve the predictions, a careful analysis of existing microseismic events is required, such as developed by the seismic density analysis.

A new geometrical far-field model needs now to be derived that includes a major flow zone between GPK3 and GPK4. The existence of such a zone is based upon three arguments: 1) there exist an aseismic zone that might be hydraulically well connected to the far-field (i.e. possibly low pressurized) and that is not suited for shear failure due to its strong E-W orientation, 2) above the open hole section of GPK4 a highly permeable zone has been intersected by drilling above the casing shoe (~4400 m) and 3) only a drainage system between GPK3 and GPK4 is suited to prevent pressurizing GPK3 when injecting GPK4 furthermore when seismicity stops its initial migration towards GPK3.

Not yet documented, further HEX-S model runs emphasize the importance of such a zone. Although they are now able to reproduce the GPK4 downhole pressure evolution and anticipate much larger time constants to pressurize adjacent boreholes, the absolute values at GPK3/GPK2 still do not fit. Further effort is needed to quantify the measured seismo-hydraulic behavior with relevant hydraulic and seismic parameters. After all, it should be emphasized that none of our models could reproduce the seismic data with a stress field changing at depth from normal to strike-slip regime. Our calculations using fracture orientations measured in the boreholes for the 5 km deep Soultz reservoir strongly support a normal stress regime.